ABSTRACT

Title of Thesis: UNDERSTANDING THE ANXIOLYTIC EFFECTS OF ALCOHOL ON THE CENTRAL EXTENDED AMYGDALA IN HUMANS

Claire M. Kaplan, Master of Science, 2017

Thesis Directed By: Dr. Alexander J. Shackman, Assistant Professor
Department of Psychology

The anxiety-reducing properties of alcohol are thought to contribute to development of alcohol dependence, particularly among individuals with anxiety disorders. Remarkably little is known, however, about the neural circuitry underlying anxiolytic effects of alcohol in humans. In a sample of 72 healthy adults, we employed the novel MultiThreat Countdown (MTC) task to investigate the dose-dependent consequences of acute alcohol intoxication (BAL range: 0.061 - 0.145%) during anticipation of certain or uncertain threat, compared to placebo. Focal analyses of the central extended amygdala revealed significant activation during threat in the right, but not left, hemisphere for both the central nucleus [Ce] and bed nucleus of the stria terminalis [BST]. Increasing BALs were associated with decreasing activation in right BST and self-reported fear/anxiety levels during threat. This effect did not differ between certain and uncertain threat. These results build upon converging lines of evidence and suggest involvement of BST in alcohol-induced anxiolysis.

UNDERSTANDING THE ANXIOLYTIC EFFECTS OF ALCOHOL ON THE CENTRAL EXTENDED AMYGDALA IN HUMANS

by

Claire M. Kaplan, B.S.

Thesis submitted to the Faculty of the Graduate School of the
University of Maryland, College Park, in partial fulfillment
of the requirements for the degree of
Master of Science
2017

Thesis Committee:
Professor Alexander J. Shackman, Chair
Professor Edward Bernat
Professor Luiz Pessoa
Professor Matthew Roesch

Collaborators: Daniel Bradford, M.S. (Wisconsin), John J. Curtin, Ph.D. (Wisconsin), and Jason F. Smith, Ph.D. (Maryland).

Acknowledgements

I am deeply grateful to my mentors, Dr. Alexander Shackman and Dr. Jason Smith, for their wise guidance and unending support throughout this project and throughout my research training. I would also like to express gratitude to my Master's Thesis committee: Drs. Bernat, Roesch, and Pessoa. Your expert advice has been crucial for the development of this project. I am especially grateful to Daniel Bradford for his generous assistance and impressive turnaround times whenever I reached out for consultation. Finally, I would like to thank my laboratory teammates, Rachael Tillman and Kathryn DeYoung, for their support and aid at various stages of the study.

Table of Contents

List of Tables

List of Figures

Chapter 1: Introduction

Alcohol misuse and abuse are a blight on both personal and public health. Alcohol misuse is common, costly, and debilitating, leading to a number of deleterious outcomes. Around the world, Alcohol Use Disorders (AUDs) are the fifth leading cause of years lost to disability; are the leading preventable cause of premature death for people aged 15 to 49; and contribute to the development of more than 200 other diseases and injury-related conditions (K. Smith, 2014). In the U.S. alone, AUDs cost roughly $250B annually ("Excessive Drinking is Draining the U.S. Economy," 2016). In short, alcohol abuse imposes a profound burden on public health and the global economy, underscoring the need to develop a better understanding of the underlying neurobiological mechanisms.

Although the transition from alcohol use to dependence is complex and involves alterations in multiple cognitive, emotional, and motivational mechanisms, a disproportionate amount of pre-clinical research has focused on alcohol's positive reinforcing effects. Yet, there is ample evidence that alcohol's negative reinforcing effects (e.g., anxiolytic and stress-dampening; relief from withdrawal-induced dysphoria) contribute to the onset, maintenance, and recurrence of problematic drinking behaviors (Cooper, 1994; Mann, Chassin, & Sher, 1987; Moberg & Curtin, 2012; Schroder & Perrine, 2007), and are particularly appreciated ('liquid courage') among individuals seeking to alleviate an anxious temperament or mood disorder (Gilpin & Koob, 2008; Schmidt, Buckner, & Keough, 2007; P. Zimmerman et al., 2003). Not surprisingly, high rates of alcohol abuse or dependence have been consistently observed in populations with anxiety disorders (Petrakis, Gonzalez, Rosenheck, & Krystal, 2002;

J. P. Smith & Randall, 2012). Yet remarkably little is known about the neural circuitry underlying the anxiolytic effects of alcohol in humans or other primates. Here, we used functional magnetic resonance imaging and a novel threat task to clarify the relevance of the central extended amygdala (i.e. anxiety-related brain regions) to the stress-dampening effects of mild-to-moderate levels of alcohol intoxication. Addressing this question is essential for determining the translational relevance of addiction models derived from mechanistic work in rodents and would inform the development of brain-based treatment strategies (Koob, 2010).

Impact of Alcohol on Signs of Fear and Anxiety in Humans

Recent psychophysiological research suggests that the emotional consequences of alcohol are robust and highly specific in humans (**Figure 1**). Across several studies, collectively incorporating several hundreds of participants, Curtin and colleagues have demonstrated that sub-sedative doses of alcohol disproportionately reduce fear and anxiety elicited by uncertain threat-of-shock in a dose-dependent manner. Moberg and Curtin (2009) first demonstrated that moderate doses of alcohol (target Blood Alcohol Level [BAL] = 0.08%) significantly reduce startle potentiation during the anticipation of uncertain, but not certain, shock delivery—a manipulation that encompasses uncertainty about whether and when the aversive reinforcement will occur. Consistent effects have since been reported in paradigms where uncertainty was established via manipulation of the timing (Hefner, Moberg, Hachiya, & Curtin, 2013), probability (Hefner & Curtin, 2012), intensity (Bradford, Shapiro, & Curtin, 2013), or somatic location (Kaye, Bradford, Magruder, & Curtin, 2017) of the shock. This selectivity has been observed using both placebo (Hefner & Curtin, 2012; Hefner et al., 2013; Moberg

& Curtin, 2009) and true no-alcohol control groups (Hefner et al., 2013). Furthermore, the anxiolytic effects of acute alcohol administration are linear across a broad range of doses (0.06 – 0.14%)—for both startle and subjective ratings of distress—in the absence of gross impairments in cognitive or motor function (Bradford et al., 2013; Kaye et al., 2017).

Neurobiology of Alcohol-Induced Anxiolysis

At these physiologically relevant concentrations (i.e. noticeable intoxication), alcohol is thought to impact neural transmission primarily by way of allosteric modulation or direct interaction with cell-surface receptors for acetylcholine (ACh), N-methyl-d-aspartate (NMDA), and gamma-aminobutyric acid (GABA-A) to alter ion transport across the cell membrane (Fadda & Rossetti, 1998). More recent studies have also identified a subtype of extrasynaptic GABA-A receptor that gives rise to tonic GABAergic inhibition as an important molecular target for alcohol, especially at such alcohol concentrations typically achieved during social alcohol ingestion (Paul, 2006). Thus, while the impact of alcohol on the central nervous system is certainly complex, its notable behavioral and emotional effects have primarily been attributed to its role as a GABA-A receptor agonist. This is further supported by studies which show that acute administration of benzodiazepines—a class of drugs which specifically increase GABA-A signaling efficiency and which are clinically effective at reducing anxiety—also selectively reduce startle potentiation during the anticipation of uncertain threat in the laboratory (Baas et al., 2002; Grillon, Baas, Pine, et al., 2006).

Mechanistic work in rodents (Breese et al., 2006; Koob, 2004, 2008; Kumar et al., 2009) , suggests that the anxiolytic effects of alcohol reflect altered GABAergic

transmission in the central extended amygdala—including the central nucleus of the amygdala (Ce) and bed nucleus of stria terminalis (BST[1]). The Ce and the BST are both well-positioned to orchestrate key features of fear and anxiety via dense projections to downstream effector regions (Davis, Walker, Miles, & Grillon, 2010; Shackman & Fox, 2016; Tovote, Fadok, & Luthi, 2015) (**Figure 2**). Moreover, these regions are marked by dense expression of GABA-A receptors (Sun & Cassell, 1993) and are sensitive to alcohol administration (Leriche, Méndez, Zimmer, & Bérod, 2008). Roberto, Madamba, Moore, Tallent, and Siggins (2003), for example, demonstrated that a single low dose of ethanol significantly increased GABA-A transmission at both pre- and post-synaptic sites in the Ce. Other work suggests that the acute anxiolytic effects of alcohol emerge from transient upregulation of GABAergic transmission in the Ce via interaction with endogenous corticotropin releasing factor (CRF) signaling (Silberman & Winder, 2015). In particular, work in rodents indicates that ethanol increases GABAergic transmission in CRF1-expressing neurons in the Ce, and that these Ce CRF1 neurons project into the BST (Herman et al., 2013). Furthermore, perturbations of the Ce-BST CRF signaling pathway—via acute administration of CRF1 antagonists or optogenetic silencing—disrupt startle responses to diffuse, uncertain threat (i.e., an aversively conditioned context) but not to acute threat (Asok, Schulkin, & Rosen, 2017; Walker et al., 2009). A crucial limitation to these rodent studies, however, is that the subjective emotional experience of the anxiolytic effects of alcohol, and thus the underlying neural mechanisms of these subjective symptoms, are impossible to assess (LeDoux, 2015).

[1] Consistent with widely used rat, monkey, and human brain atlases—(Mai, Majtanik, & Paxinos, 2015; Paxinos, Huang, Petrides, & Toga, 2009; Paxinos & Watson, 2014)—including that recently developed by the Allen Brain Institute (http://www.brain-map.org)—we use the acronym 'BST' (rather than 'BNST') to refer to the bed nucleus of the stria terminalis.

At present, the relevance of the central extended amygdala to the stress-dampening effects of alcohol in humans remains little explored and poorly understood. To date, human imaging studies have focused on emotional face paradigms, showing that acute alcohol administration reduces amygdala reactivity to threat-related expressions (Bjork & Gilman, 2014; Sripada, Angstadt, McNamara, King, & Phan, 2011). This may reflect alterations in GABAergic transmission, given evidence that benzodiazepine administration produces a dose-dependent reduction in amygdala reactivity to emotional faces (Paulus, Feinstein, Castillo, Simmons, and Stein (2005). Although these insights are important, the mere presentation of still photographs of threat-related faces is not sufficient to elicit fear and anxiety (Shackman et al., 2016; Shackman et al., 2006). Thus, the relevance of the extended amygdala to alcohol-induced anxiolysis in humans or the selectivity of such effects to uncertain threat is unknown. Addressing these questions is important and promises to inform our understanding of the mechanisms underlying alcohol use and abuse.

Chapter 2: Present Study

Overview of Approach

Here, we used multiband fMRI and a novel 'MultiThreat Countdown' (MTC) task to determine the dose-dependent consequences of acute alcohol intoxication during the anticipation of certain or uncertain threat in the Ce and BST. Healthy young adults were randomly assigned to receive low to moderate doses of alcohol (BAL 0.06 - 0.14%) or placebo beverages (single blind) in a single-session, between-subjects design. Building on prior psychophysiological and imaging research (Kaye et al., 2017; Somerville et al., 2013), the MTC task took the form of a 2 (Valence: Safe, Threat) × 2 (Certainty: Certain, Uncertain) design embodied in a rapid, fully randomized event-related trial structure (**Figure 3**). Subjects anticipated the delivery of neutral or aversive stimuli ('count-down' period), where the timing of delivery was either certain or uncertain. To maximize fear and anxiety, on Threat trials, the anticipatory period terminated with the delivery of shock, an unpleasant image (e.g., mutilated body), and a thematically related auditory cue (e.g., gunshot and scream). The MTC task has a number of advantages over alternative designs (e.g., enhanced matching of signal variance and perceptual inputs; cf. Shackman & Fox, 2016; Hefner et al., 2013). BAL was estimated immediately before and after scanning using a breath assay. During the MTC task, subjective ratings of anxiety/fear were acquired on-line for each condition type, consistent with recent recommendations (Grillon, Baas, Pine, et al., 2006).

Hypotheses

Our approach afforded the opportunity to test several key predictions.

Prediction 1: Based on prior psychophysiological research (Bradford et al., 2013; Grillon, Baas, Cornwell, & Johnson, 2006), we predicted that alcohol will disproportionately reduce distress elicited by Uncertain relative to Certain Threat (i.e., Certainty × Valence × Alcohol interaction)

Prediction 2: We tested several competing predictions about the consequences of Threat for activation in the Ce and BST. Among researchers focused on humans, it is widely believed that the Ce and BST are functionally dissociable (Shackman & Fox, 2016; Shackman et al., 2016). Inspired by an earlier generation of mechanistic work in rodents (Davis, 2006), this model suggests that the Ce triggers transient defensive responses to certain threat (e.g., Pavlovian threat cues), whereas the BST orchestrates defensive responses during sustained exposure to dangers that are uncertain, psychologically diffuse, or temporally remote (e.g., open-field, elevated plus-maze, Pavlovian threat contexts)[2]. Several human imaging studies have reported evidence consistent with this hypothesis (Alvarez, Chen, Bodurka, Kaplan, & Grillon, 2011; Brinkmann et al., 2017; Herrmann et al., 2016; McMenamin, Langeslag, Sirbu, Padmala, & Pessoa, 2014; Somerville et al., 2013). This work motivates the hypothesis that the Ce will be more responsive to Certain Threat, whereas the BST will be more

[2] This hypothesis has been adopted by numerous investigators and theorists (Avery, Clauss, & Blackford, 2016; Grupe & Nitschke, 2013; Lebow & Chen, *in press;* LeDoux, 2015) and enshrined in the National Institute of Mental Health (NIMH) Research Domain Criteria (RDoC) as *Acute Threat* and *Potential Threat* (e.g., https://www.nimh.nih.gov/research-priorities/rdoc/constructs/acute-threat-fear.shtml; https://www.nimh.nih.gov/research-priorities/rdoc/constructs/potential-threat-anxiety.shtml; https://www.nimh.nih.gov/research-priorities/rdoc/negative-valence-systems-workshop-proceedings.shtml).

responsive to Uncertain Threat, manifesting as a Valence × Certainty × Region interaction.

On the other hand, converging evidence from studies of rodents, monkeys, and humans suggests that the Ce and BST are similarly involved in orchestrating responses to a wide range of threats (Gungor & Paré, 2016; Shackman & Fox, 2016). Mechanistic work in rodents suggests that both regions play a critical role in assembling defensive responses to diffuse threatening contexts (Botta et al., 2015; Duvarci, Bauer, & Paré, 2009; Jennings et al., 2013; Kim et al., 2013; Moreira, Masson, Carvalho, & Brandao, 2007; J. M. Zimmerman & Maren, 2011; J. M. Zimmerman, Rabinak, McLachlan, & Maren, 2007) and, although it remains underappreciated, Davis and colleagues reformulated their model nearly a decade ago to suggest that the Ce responds to both certain/cued and uncertain/contextual threats, whereas the BST selectively responds to uncertain/contextual threat (Davis et al., 2010). Consistent with this possibility, human imaging studies have observed elevated activation in the dorsal amygdala during the anticipation of uncertain threat (Andreatta et al., 2015; Lieberman, Gorka, Shankman, & Phan, 2017; Williams et al., 2015). Other work has revealed phasic responses in the BST to brief (4-s) cues signaling the certain delivery of noxious shock (Klumpers et al., 2015), consistent with evidence from recording studies in rodents (Gungor & Paré, 2016). On balance, this body of evidence suggests the Ce and BST are more alike than different, motivating the hypothesis that both regions will be similarly responsive.

Prediction 3: Given evidence that alcohol and benzodiazepine administration disproportionately dampens psychophysiological signs of anxiety during Uncertain Threat (Baas et al., 2002; Bradford et al., 2013; Grillon, Baas, Pine, et al., 2006; Kaye et

al., 2017), we predict that alcohol will disproportionately dampen the blood oxygen level-dependent (BOLD) response in regions sensitive to Uncertain Threat. As with Prediction 2, we entertained competing predictions about the regional consequences of these effects. If the central extended amygdala is indeed strictly segregated (Davis, 2006), with selective engagement of the BST by Uncertain Threat, we expect a regionally specific dose-dependent reduction in activation (i.e., Valence × Certainty × Region × BAL). On the other hand, if the Ce and BST both play a role in responding to Uncertain Threat (Shackman & Fox, 2016; Davis et al. 2010; Gungor & Paré, 2016), then we expect reduced activation across the extended amygdala during threat anticipation (i.e., Valence × BAL).

Chapter 3: Methods

Participants

Participants included 87 adults between the ages of 21 and 35 years recruited from the local community. All had experience with the highest study dose of alcohol used in the present study (~4-5 standard drinks) within the past 12 months, and self-reported the absence of alcohol-related problems, current psychiatric diagnosis or treatment, and a medical condition that would contraindicate alcohol consumption or MRI. Exclusion criteria also included a self-reported history of neurological symptoms. Fifteen participants were excluded from analyses due to excessive drowsiness (*N*=5), incidental neurological findings (*N*=3), difficulty complying with task instructions (*N*=4), technical issues with the electrical stimulator (*N*=2), or generalized discomfort in the scanner (*N*=1). Thus, a total of 72 participants contributed data to one or more analyses (i.e., fMRI and/or Ratings; see **Table 1** for characteristics of total sample). Of these, five participants were excluded from fMRI analyses due to unusable T1-weighted datasets (*N*=3), excessive motion artifact (*N*=1), or technical problems with the scanner (*N*=1), yielding a final imaging sample of 67 participants (33 females). For ratings analyses, eleven participants were excluded from analyses due to invariant ratings, yielding a final ratings sample of 61 participants (34 females). Demographic characteristics of the fMRI and Ratings samples can be found in the Appendix.

Self-Report Measures

Drinking habits (e.g. retrospective summary of quantity and frequency of alcohol use) were assessed using the Quick Drinking Screen (QDS) (Sobell et al., 2003).

Blood Alcohol Level (BAL) manipulation

The BAL manipulation was adapted from techniques established and refined by Curtin and colleagues (Bradford et al., 2013; Hefner & Curtin, 2012). Participants were randomly assigned, within sex and race/ethnicity, to receive either alcohol or a placebo beverage. Doses within the Alcohol group were titrated to achieve a target BAL of 0.08% or 0.12% with an expected variance of approximately ±0.02%. As shown in **Figure 4**, these procedures produced a continuous, unimodal distribution (*M* = .093%, *SD* = 0.02%, Range: 0.061% to 0.146%).

Participants were instructed to abstain from alcohol and other drugs for at least 24 hours and from all food for at least 3 hours prior to the imaging session. Regardless of group assignment, all participants were informed that they could receive a moderately impairing dose of alcohol. To verify initial sobriety, participants completed a standard breath assay at the start of the session (Alcosensor IV Breathalyzer; Intoximeters Inc., St. Louis, MO), and those with an estimated BAL > 0.00% were dismissed (*N*=1). Prior to scanning, participants assigned to the Alcohol group were given a titrated dose of alcohol using a well-established formula that accounts for individual differences in height, weight, age, and sex to produce a specified target BAL ~30 minutes after the completion of beverage consumption (for additional details, please see Curtin & Fairchild, 2003). Doses within the Alcohol beverage group were titrated to achieve a target BAL of 0.08% or 0.12% with an anticipated variance of +/- 0.02%. This produced a unimodal distribution of mean BAL (range: 0.061% - 0.145%). Alcoholic beverages contained a mixture of cranberry juice, Tang™, and 100-proof vodka (Smirnoff Blue™). To ensure controlled absorption rates, participants consumed

3 equal doses, evenly spaced over 30 minutes. Participants in the Placebo group received a similar beverage, with an equivalent volume of distilled water replacing the vodka. The placebo manipulation[3] was reinforced by floating 3 ml of Peychaud's bitters and 3 ml of vodka on the surface of the beverage and delivering a minute amount of aerosolized vodka to the rim of the beverage containers. All beverages were prepared in a separate room, out of the subject's view. Immediately following consumption of the third beverage, BAL was assessed and subjects were scanned (latency from pre-MRI breath assay to the first functional task EPI scan: M = 33.5 min, SD = 8.5 min). BAL was re-assessed immediately following the final scan (inter-assessment period: M = 70.9 min, SD = 8.0 min). Hypothesis testing employed the mean BAL across the pre- and post-scanning assays. Subjects who consumed alcohol were required to remain at the imaging center until their estimated BAL was <0.03%.

Scanning and muscle stimulation procedures

Prior to beverage consumption, participants were informed of the four condition types (Certain vs Uncertain Threat, and Certain vs Uncertain Safe; **Figure 3**), but received no specific information about the duration of the anticipatory ('count-down') period for Uncertain trials. Visual stimuli were presented using Presentation software (Neurobehavioral Systems) and viewed on a projection screen in the MRI scanner using a mirror mounted to the head coil. On the left hand, MRI-compatible electrodes were affixed to the fourth and fifth phalanges for electric muscle stimulation delivery (Coulbourn Instruments; duration = 500 ms) during scanning. Shock intensity was

[3] The placebo manipulation proved effective. At the end of the session, subjects randomly assigned to the Placebo group reported consuming an average of 2.2 standard drinks (SD = 1.2, Range = 0–5 drinks) prior to debriefing, significantly greater than zero ($t(22) = 9.0$, $p < 0.001$). Participants in the Alcohol group reported a mean of 4.5 drinks in their beverage (SD = 1.4, Range = 2–8 drinks).

calibrated for each participant immediately before functional imaging by asking them to select a stimulation level that was the "most unpleasant you are willing to tolerate for the purposes of the experiment." Fear/anxiety ratings were collected on-line using an MRI-compatible response device.

MTC Task

Building on mechanistic work in rodents (Davis et al., 2010) and psychophysiological and imaging research in humans (Hefner et al., 2013; Somerville et al., 2013), the MTC task took the form of a 2 (Valence: Safe, Threat) × 2 (Certainty: Certain, Uncertain) design embodied in a rapid, fully randomized event-related trial structure (**Figure 3**). On each trial, subjects anticipated the delivery of neutral or threatening stimuli ('count-down' period), where the timing of delivery was either certain or uncertain. On Certain trials, the number of seconds remaining in the anticipatory period was continuously and reliably signaled by a visual train of integers presented in sequential order (i.e., 18, 17, 16…3, 2, 1). On Uncertain trials, the duration of the anticipatory period was highly (Range: 8 – 30 s, M = 18 s) and the integers were presented in a pseudo-randomized order. On both Certain and Uncertain trials, the valence of the upcoming reinforcer was unambiguously signaled throughout the anticipatory period by the background color of the display (Threat = red, Safe = blue). To maximize threat intensity and subject engagement, stimulus-unique combinations of noxious shock, aversive images, and unpleasant sounds served as the aversive reinforcer (i.e., 'MultiThreat'). Aversive images were selected from the International Affective Picture System (IAPS) (Lang, Bradley, & Cuthbert, 2008).

The task consisted of 6 trials per condition, for a total of 24 trials, with an inter-trial interval of 1 s. Trials were presented in a pseudo-random order. Time series simulations were used to minimize collinearity (estimated VIFs = 1.10 – 1.67). Participants were also prompted to provide on-line ratings of subjective fear/anxiety level. Four prompts were delivered, one for each trial type. Ratings were made on a 1 (*least*) to 4 (*most*) scale and were referenced to anticipatory period of the prior trial. Data for the MTC task were collected prior to a larger battery of imaging tasks.

MRI Data Acquisition

Imaging data were collected on a 3T Siemens TIM Trio scanner equipped with a 32-channel head coil. Sagittal T1 weighted anatomical images were acquired using a magnetization-prepared, rapid-acquisition, gradient-echo sequence (TR = 1900 ms; TE = 2.32 ms; inversion time = 900 ms; flip angle = 9°; sagittal slice thickness = 0.9 mm; voxel size in plane = 0.449 × 0.449mm; matrix = 512 × 512; field of view = 230 × 230). To enable fieldmap distortion correction, a pair of oblique-axial co-planar spin echo images with opposing phase encoding direction were acquired (TR = 7220 ms; TE = 73 ms; slice thickness = 2.2 mm; matrix = 96 × 96). A total of 568 oblique-axial EPI volumes were collected during the MTC task scan (multiband acceleration = 6; TR = 1000 ms; TE = 39.4 ms; flip angle = 90°; slice thickness = 2.2 mm, number of slices = 60; voxel size in-plane = 2.1875 x 2.1875 mm; matrix = 96 × 96). Images were collected in the oblique axial plane (approximately -20°relative to the ACPC plane) to minimize susceptibility artifacts.

MRI Data Preprocessing

The first 3 volumes of each EPI functional task scan were removed to allow for equilibrium, and the remaining volumes were de-spiked and slice-time corrected using AFNI (Cox, 1996). T1 images were inhomogeneity-corrected with N4 (Tustison et al., 2010) and diffeomorphically normalized to the 1-mm MNI152 template using ANTS (Avants et al., 2011). The N4 image was skull-stripped and segmented in FSL (S. M. Smith et al., 2004). The first remaining volume of the EPI images was then co-registered to the anatomical T1 weighted images using the boundary-based registration approach (with fieldmap correction) implemented in FSL (Greve & Fischl, 2009). The EPI to T1 transform was converted to ITK format (Insight Segmentation and Registration Toolkit; Yoo et al., 2002) for use with ANTS. To minimize spatial blurring, the transformation matrices for affine motion correction, co-registration, and spatial normalization to the MNI152 template were concatenated and applied to the EPI data in a single step. Normalized EPI data were resampled to 2-mm isotropic voxels using 5^{th}-order splines and smoothed (6 mm FWHM). To attenuate physiological noise, white matter (WM) and cerebrospinal fluid (CSF) time-series were extracted from the spatially unsmoothed, normalized EPI data. WM and CSF compartments were identified using the probabilistic segmented images provided with the MNI152 template. All datasets were visually inspected for quality assurance. To assess residual motion artifacts, the number of volumes with >0.5mm volume-to-volume displacement of a selected voxel in the anterior cingulate cortex [5, 34, 28] was calculated using the motion-corrected EPI data. Datasets where >5% of the volumes met this criterion were excluded from analyses (N=1).

Ce and BST Regions of Interest (ROIs)

Building on prior work by our group using similar methods (Birn et al., 2014; Nacewicz, Alexander, Kalin, & Davidson, 2014; Oler et al., 2012; Oler et al., 2017), the Ce was manually prescribed by a trained neuroanatomist (Dr. B. M. Nacewicz, Department of Psychiatry, University of Wisconsin—Madison; (cf. Nacewicz et al., 2014) based on the atlas of Mai and colleagues (Mai, Paxinos, & Voss, 2007; Prevost, McCabe, Jessup, Bossaerts, & O'Doherty, 2011) using a specially processed high-resolution (0.7-mm), multimodal (T1/T2) probabilistic template (Tyszka & Pauli, 2016) (**Figure 5a**) [4] . The BST ROI was implemented using a previously published probabilistic region of interest (Theiss, Ridgewell, McHugo, Heckers, & Blackford, 2016) (**Figure 5b**). Both ROIs were decimated to the 2-mm MNI template. Decimation was performed using an iterative procedure that maintained a consistent seed volume across templates. Each seed was minimally smoothed using a Gaussian kernel and the voxel size was dilated by 0.1-mm and resliced (linear interpolation), enabling us to identify a threshold that matched the original seed volume as closely as possible.

[4] The criteria used for manually prescribing the Ce seed represent an extension of our previously published protocol (Nacewicz et al., 2006; for recent applications, see Chung et al., 2010; Dalton et al., 2006; Hanson et al., 2012, 2015) and leverages the additional contrast afforded by the high-resolution, multimodal template. In contrast to other recent work (Birn et al., 2014; Oler et al., 2012; Tyszka & Pauli, 2016), the Ce was manually prescribed in both the left and right hemispheres. The criteria were derived from the atlas of Mai and colleagues (2007) and hinged on identifying the lateral division of the Ce (CeL) at its first appearance caudally and including surrounding tissue up to the boundary with the ventral putamen (laterally and dorsally) and the more T1-intense basolateral nuclei (ventrally). Moving rostrally, a thin, notch-like band of white matter separates the dorsal portions of the basolateral and lateral nuclei from the Ce. The ventromedial tip of the white matter separating the Ce from the basolateral nuclei was then followed in a straight line to the lateral margin of the optic tract or the rhinal sulcus to form the ventromedial border. A major landmark is the disappearance of the head of the hippocampus, at which point the CeL can no longer be discerned. The Ce curves medially and ventrally during the progression from caudal to rostral slices, and in the sections rostral to the disappearance of the hippocampus, care was taken not to include the peri-amygdalar claustrum (lateral to the Ce). In the middle and rostral slices, portions of the boundary between the Ce and medial nuclei was not evident in the T1 and T2 templates. In these cases, the visible portions of the boundary were extrapolated using straight lines. Preliminary traces were refined in all three cardinal planes. In the case of conflicting traces, the axial and coronal slices were favored over the more variable sagittal slice.

Chapter 4: Data Analysis

Data reduction and first-level (single-subject) modeling

First-level modeling was performed using SPM12 (http://www.fil.ion.ucl.ac.uk/spm) and in-house MATLAB code. Using a duration-modulated variable boxcar function convolved with a canonical hemodynamic response function (HRF), activation during the anticipatory ('count-down') period was separately modeled for the Certain-Threat (CT), Uncertain-Threat (UT), and Uncertain-Safe (US) conditions, with Certain-Safe (CS) serving as an implicit baseline. Aversive reinforcers, neutral reinforcers, and rating prompts were modeled using a similar approach. Nuisance variates included motion estimates and physiological noise (i.e., WM/CSF signals). Regression coefficients were extracted for each of the four trial types for each subject and averaged across voxels separately for the left and right Ce and BST ROIs.

Hypothesis testing at the second-level (group analyses)

Omnibus mixed-model general linear models were computed using SPSS (24.0.0.0). Analyses of ratings and imaging data were broadly similar and both incorporated Valence (Safe, Threat), Certainty (Certain, Uncertain), and individual differences in mean-centered average BAL. Analyses of imaging data also included Region (Ce, BST) and Hemisphere (Left, Right) as repeated-measures factors. Significant interactions were decomposed using focal tests of the mean differences or association with BAL. Figures were generated using RStudio (RStudio: Integrated development environment for R, 2017) for R (R Development Core Team, 2017).

Chapter 5: Results

Acute alcohol intoxication reduces threat-elicited subjective fear/anxiety

Participants (N = 61) retrospectively reported significantly greater fear/anxiety during the anticipatory period of Uncertain compared to Certain trials ($F(1,59) = 15.78$, $p < .001$) and during Threat compared to Safe trials ($F(1,59) = 65.43$, $p < .001$) (**Table 2** and **Figure 6**). The valence effect was significantly stronger on Certain compared to Uncertain trials (Valence × Certainty: $F(1,59) = 3.96$, $p = .05$). Higher blood alcohol levels were associated with a selective dampening of fear/anxiety during the anticipation of Threat trials ($r_{Threat} = -.28$, $p = .03$; $r_{Safe} = -.03$, $p = .83$; $r_{Threat\text{-}Safe} = -.23$, $p = .07$; Valence × BAL: $F(1,59) = 3.34$, $p = .07$) (**Figure 7**). The anxiolytic effects of alcohol remained significant after controlling for a range of potential nuisance variates, including mean-centered age, sex, weekly alcohol consumption, or the latency between the time of alcohol consumption and the beginning of the first functional scan (ps = .02-.05). In short, the MTC task reliably elicits feelings of fear and anxiety and higher levels of alcohol are associated with a dose-dependent reduction in this threat-elicited distress. Consistent with prior work (Grillon, Baas, Pine, et al., 2006), we failed to uncover evidence that alcohol-induced anxiolysis is selective to Uncertain Threat. No other effects were significant, ps > .05[5].

[5] Skin conductance data were acquired throughout each scan, filtered, and averaged separately for each trial type. Across a range of data-processing approaches and outlier-rejection techniques, we consistently observed significant threat-induced elevations in arousal, indexed by skin conductance levels (SCL; ns = 71-68; ps < .05). This dovetails with prior work employing threat-of-shock paradigms (e.g. McMenamin et al., 2014) and indicates that the MTC paradigm successfully elicited objective signs of fear and anxiety. Nevertheless, because the influence of Certainty and BAL was inconsistent across approaches, we refrain from reporting or interpreting more nuanced effects.

BOLD responses in Ce and BST are heightened by threat, and BST is dampened by alcohol

An omnibus mixed-model GLM revealed greater activation, on average, during Threat compared to Safe trials (M_{Safe} = -.019, SE_{Safe} = .012; M_{Threat} = 0.022, SE_{Threat} = .020; Valence: $F(1,64) = 4.78$, $p = .03$). The magnitude of this valence effect was stronger in the Ce compared to the BST (M_{Ce} =.065, SE_{Ce} = .028; M_{BST} = .018, SE_{BST} = .014; Valence × Region: $F(1,64) = 4.16$, $p = .05$), and conditional on Hemisphere, Certainty, and BAL (Valence × Region × Hemisphere × BAL: $F(1,64) = 8.05$, $p = .006$; Valence × Certainty × Hemisphere: $F(1,64) = 4.11$, $p = .05$; other omnibus effects were not significant, ps > .05). To decompose this complexity, separate analyses were conducted for each Region[6].

Analyses focused on the Ce revealed significantly greater activation on Certain compared to Uncertain trials ($M_{Certain}$ = .020, $SE_{Certain}$ = .018; $M_{Uncertain}$ = -.026, $SE_{Uncertain}$ = .028; Certainty: $F(1,64) = 4.19$, $p = .05$) and on Threat compared to Safe trials ((M_{Threat} = .03, SE_{Threat} = .031; M_{Safe} = -.035, SE_{Safe} = .016; Valence: $F(1,64) = 5.45$, $p = .02$) (**Figure 8**). Although the valance effect was qualified by a significant Valence × Hemisphere × BAL interaction ($F(1,64) = 4.47$, $p = .04$), focal analyses failed to uncover reliable associations with BAL in either hemisphere (Left Ce: $r_{Threat-Safe}$ = -.14, $p = .25$; Right Ce: $r_{Threat-Safe}$ = .18, p = .15). No other omnibus effects were

[6] Given recent interest in understanding the degree to which the Ce and BST are marked by dissociable functional profiles (e.g., Shackman & Fox, 2016; Gorka, Torrisi, Shackman et al., in press), we directly tested the degree to which the valence effect (i.e., Threat vs. Safe) differed across regions, when considering each hemisphere separately. For the right hemisphere, both regions showed significant valence effects (Fs(1,64) = 5.87-6.08, ps = .02) and the size of this effect did not differ across regions ($F(1,64) < 1$, $p = .36$), whereas for the left hemisphere, neither region showed significant valence effects (Fs(1,64) = .047-3.32, ps = .83-.07). These observations are consistent with the possibility that the Ce and BST are more alike than different.

significant in the Ce (*p*s > .05). In sum, the Ce shows elevated activation during the anticipation of certain outcomes and threat. We found no evidence that the magnitude of threat-elicited activation in the Ce is moderated by the temporal certainty of threat delivery or BAL.

In the BST, the influence of threat was conditional on both Hemisphere and Certainty (Valence x Hemisphere: $F(1,64) = 6.34$, $p = .01$; Valence x Certainty x Hemisphere: $F(1,64) = 6.42$, $p = .01$). These effects were decomposed using focal analyses computed separately for each hemisphere. Those focused on the right BST revealed significantly greater activation during the anticipatory period of Threat compared to Safe trials (M_{Safe} =-.013, SE_{Safe} =.012; M_{Threat} =.026, SE_{Threat} =.017; Valence: $F(1,64) = 6.08$, $p = .02$) (**Figure 8**). The magnitude of this valence effect was significantly reduced in individuals with higher BALs ($r_{Threat\text{-}Safe}$ = -.25, $p = .05$; Valence × BAL: $F(1,64) = 4.19$, $p = .04$) (**Figure 9**). This linear dose-response relationship remained significant after controlling for a range of potential nuisance variates, including mean-centered age, sex, weekly alcohol consumption, or the latency between the time of alcohol consumption and the beginning of the first functional scan (*p*s = .04-.05). No other omnibus effects were significant in the right BST and analyses focused on the left BST failed to uncover significant effects (*p*s > .05). Together, these observations indicate that activation in the right BST is elevated by threat and dampened by alcohol. As with the Ce, we found no evidence to suggest that the BST is disproportionately sensitive to Uncertain Threat.

Chapter 6: Discussion

These results suggest that acute alcohol administration exerts a non-specific dampening effect for both temporally certain and uncertain threat, as indicated by subjective measures of fear/anxiety ratings and BOLD responses in the central amygdala and bed nucleus of the stria terminalis. Consistent with Grillon, Baas, Pine, et al. (2006), participants reported greater levels of fear/anxiety during Certain Threat as well as a dose-dependent reduction in threat-elicited fear/anxiety, however the interaction of BAL and threat-certainty was not significant for distress.

Likewise, imaging analyses revealed that both the Ce and right BST show heightened BOLD response to Threat trials. Although the Ce was more sensitive to Certain (vs Uncertain) Threat, there were no significant differences between the Ce and BST for threat-certainty. Furthermore, there was a non-specific dose-dependent dampening of this valence effect (i.e. Threat vs Safe) by alcohol in the right BST.

Collectively, these observations have potentially important implications for our understanding of fear and anxiety and may offer new insights into the stress-dampening/anxiolytic effects of acute alcohol intoxication. First, our findings suggest that the Ce and BST may be more broadly alike than dissimilar during anticipation of threat, consistent with Shackman and Fox (2016). Both regions exhibited overall heightened sensitivity to threat, while the null interaction of Region × Valence × Certainty indicates similar responses to threat-certainty. This is a particularly compelling observation for several reasons—considering the use of *a priori* ROI's to reduce bias and enhance power, as well as following a formal test procedure of the appropriate interactions (see also Fox, Lapate, Shackman, & Davidson, *in press*).

Moreover, as these analyses were conducted on signals extracted over the full time-course of the countdown periods (Certain = 18s; Uncertain: *M* = 18 s, Range = 8 – 30 s), these findings may also serve to clarify the distinction between threat certainty and threat latency, which are often confounded in threat-of-shock paradigms that alternate between brief cues and prolonged contexts to assess certain vs uncertain threat[7].

In contrast to psychophysiology studies of startle potentiation, our results indicate that alcohol-induced distress dampening is not selective for uncertain threat. This may be influenced by several factors—namely the inherently retrospective nature of subjective assessment measures, and the lengthier time-course of MTC task trials and regional BOLD responses. Indeed, while substantial evidence suggests the amygdala is a critical mediator for defensive response mobilization as indexed by startle potentiation (Buchanan, Tranel, & Adolphs, 2004; Davis, 2000; Funayama, Grillon, Davis, & Phelps, 2001), several imaging studies have failed to associate startle potentiation with BOLD response in this region during various acute (e.g. aversive images) and uncertain threat-of-shock paradigms (Gorka, Lieberman, Shankman, & Phan, 2017; Wendt, Lotze, Weike, Hosten, & Hamm, 2008). Thus, while it is certainly well-evidenced that alcohol selectively dampens startle potentiation to uncertain but not certain threat, we did not find a similar pattern for BOLD response in the Ce or BST.

Our findings also indicate that the influence of alcohol may be regionally selective within the central extended amygdala. We observed a significant interaction of

[7] There is compelling evidence that multiple dimensions of threat—probability, imminence (i.e., physical distance or temporal latency), and duration—are relevant to the development of anxiety and substance abuse (Shackman et al., 2016). Yet, we know remarkably little about how the brain represents and differentially responds to them. Although important strides have been made (Shackman & Fox, 2016), conceptual progress has been slowed by the use of task paradigms that confound these key dimensions (e.g., *if* vs. *when* threat will occur; brief cues vs. prolonged contexts) or other perceptual characteristics (e.g., emotional faces vs. threat-of-shock). With this in mind, we developed the MTC task to assess responses to threat within the dimension of temporal certainty.

Valence × Region × Hemisphere × BAL, such that only the right BST showed evidence of dose-dependent reductions in threat-elicited activation. This raises some important questions regarding the potential importance of the BST as a pharmacological target for anxiolytic compounds, however future investigations are needed to further clarify this result in the context of whole-brain and behavior (see *Future Challenges* for more details).

Conclusions

Here, we see that the novel MultiThreat Countdown task reliably elicits subjective fear/anxiety during Threat compared to Safe trials, that this is conditional on Certainty, and that higher blood alcohol levels are associated with a dose-dependent reduction in threat-elicited distress. Both *a priori* regions—the Ce and BST—show elevated BOLD response during the anticipation of threat, and we failed to find evidence suggesting a disproportionate sensitivity to Uncertain compared to Certain Threat in either region. Focal analyses further revealed that while the Ce is more sensitive to temporally certain (vs uncertain) threat, the right BST showed a dose-dependent reduction of threat-elicited activation not conditional on certainty. These results demonstrate that mild to moderate doses of alcohol alters subjective distress and BOLD response in the extended amygdala during anticipation of threat, however, contrary to psychophysiology research, these measures do not reveal a disproportionate effect of alcohol on certainty during threat. Further investigation is warranted to clarify these differences.

Overall, this study provides new insights into the impact of acute alcohol intoxication on the neural mechanisms of the Ce and BST during certain and uncertain

threat in humans, and underscores the value of the MultiThreat Countdown task to help set the stage for efforts to develop more integrative bidirectional translational models to better understand mechanisms underlying anxiety and substance abuse.

Chapter 7: Future Challenges

While the current study offers interesting results, a number of important questions about the nature of these neural mechanisms and how they relate to behavior remain unanswered. Here, we highlight several crucial questions and outline some strategies for addressing them.

Assessing temporal dynamics of the Ce and BST by condition

Rodent work also motivates a hypothesis, originally proposed by Davis (1998), which dissociates the Ce and BST with regards to the time course of activation to different types of threat cue information—whereby acute/specific threat cue information has been shown to trigger phasic Ce activation, the BST is argued to respond for lengthier, sustained periods to uncertain/diffuse information. While several imaging studies in humans have since provided supporting evidence for Davis' hypothesis, claiming transient hemodynamic responses in the dorsal amygdala in response to clear and imminent threat cues, such as shock or aversive images, while showing more persistent sustained responses in the BST during uncertain anticipation of these noxious stimuli (e.g. Somerville et al., 2013), many have used more traditional modeling methods (e.g. canonical HRFs) which do not allow for strong claims regarding specific temporal dynamics over time. A key challenge for future directions will be to use finite impulse response (FIR) or related approaches to assess temporal dynamics across the count-down period of our trials and quantify momentary changes in the BOLD signal, as in some prior work. For example, Andreatta et al. (2015) used a finite impulse response (FIR) approach to demonstrate sustained activation in the region of the Ce during exposure to a virtual-reality context (30-sec) paired with unpredictable electric

shocks. The design of the MTC task offers a critical opportunity to assess the temporal dynamics of the Ce and BST using an FIR-type approach, given the nature and duration of the trials. Lastly, given that many temporally protracted processes—such as those elicited during the countdown periods of our task—may be associated with variable BOLD responses that cannot be effectively captured by the canonical HRF set (Lindquist, Loh, Atlas, & Wager, 2009), finite impulse response (FIR) basis functions can serve to more effectively capture these phasic vs sustained signals.

Investigating whole-brain effects and measures of functional connectivity

While our ROI-based approach has a number of strengths, including enhanced power and reduced bias, it is not without notable limitations. First, the use of spatially unsmoothed data would enhance spatial resolution and strengthen our confidence that the signals measured in the Ce and BST do not reflect 'roll-off' from neighboring regions. Second, it is likely that fear and anxiety – and the stress dampening effects of alcohol – reflect the coordinated interactions of larger brain networks, not isolated brain regions. As such, whole-brain analyses would afford important opportunities for determining the consequences of alcohol on the large-scale brain networks thought to underlie fear and anxiety. For example, McMenamin et al. (2014) demonstrated that states of heightened anxiety leads to alterations in network communication between the BST, anterior insula (AI), and mid-cingulate cortex (MCC). From the current study, it would be of interest to determine whether the anxiolytic effects of alcohol impact a larger network of brain regions, relative to changes in the BST.

Identify regions that mediate the anxiolytic effects of alcohol

Our conclusions reflect separate analyses of subjective distress and brain function however it will be important to link these measures for a more comprehensive understanding of brain and behavior. Thus, a key challenge for the future will be to develop more integrative analytic approaches (e.g. Atlas, Bolger, Lindquist, & Wager, 2010; Lim, Padmala, & Pessoa, 2009) that can be used to directly identify brain regions mediating the anxiolytic effects of alcohol. As noted in Grillon, Baas, Pine, et al. (2006), such analyses linking subjective ratings to BOLD response may critically depend on the psychometric properties of the measures. To increase reliability, it will be useful to more frequently probe distress during the task (e.g., at the end of each trial), as well as include several catch-trials which would potentially reduce retrospective bias.

Tables

Table 1

Total sample characteristics (N=72)

Variable	Total	Placebo	Alcohol	*P*-value
Sample size (*N*)	72	23	49	
Age (years)	22.2 (2.12)	22.2 (1.34)	22.2(2.42)	t(70) = 0.2, *p* = 0.9
Gender				
Female	53% (*n*=38)	48% (*n*=11)	55% (*n*=27)	z = -0.6, *p* = 0.6
Male	47% (*n*=34)	52% (*n*=12)	45% (*n*=22)	
Current Alcohol Use				
Mean drinks/week	7.31 (6.39)	7.0 (5.84)	7.46 (6.68)	t(50) = 0.3, *p* = 0.8
BAL (%)				
Prior MRI session	0.095 (0.02)	0.002 (0.00)	0.106 (0.08)	t(60) = 30, *p*<0.001*
After MRI session	0.092 (0.02)	0.00 (0.00)	0.093 (0.02)	t(50) = 30, *p*<0.001*

Note: Placebo and Alcohol group characteristics were tested for differences using Welch's unpaired t-test to account for unequal variances between groups. Equality of gender proportions were testing using a binomial GLM.

Table 2

Mean (SD) Fear/Anxiety Ratings in each Condition by Group

Trial type	Total	Placebo	Alcohol
Threat	2.44 (0.72)	2.68 (0.84)	2.32 (0.64)
Uncertain Threat (UT)	2.51 (0.91)	2.84 (0.96)	2.37 (0.88)
Certain Threat (CT)	2.36 (0.81)	2.53 (0.91)	2.28 (0.77)
Safe	1.62 (0.56)	1.61 (0.52)	1.63 (0.58)
Uncertain Safe (US)	1.84 (0.70)	1.89 (0.74)	1.82 (0.70)
Certain Safe (CS)	1.40 (0.58)	1.32 (0.48)	1.43 (0.62)

Figures

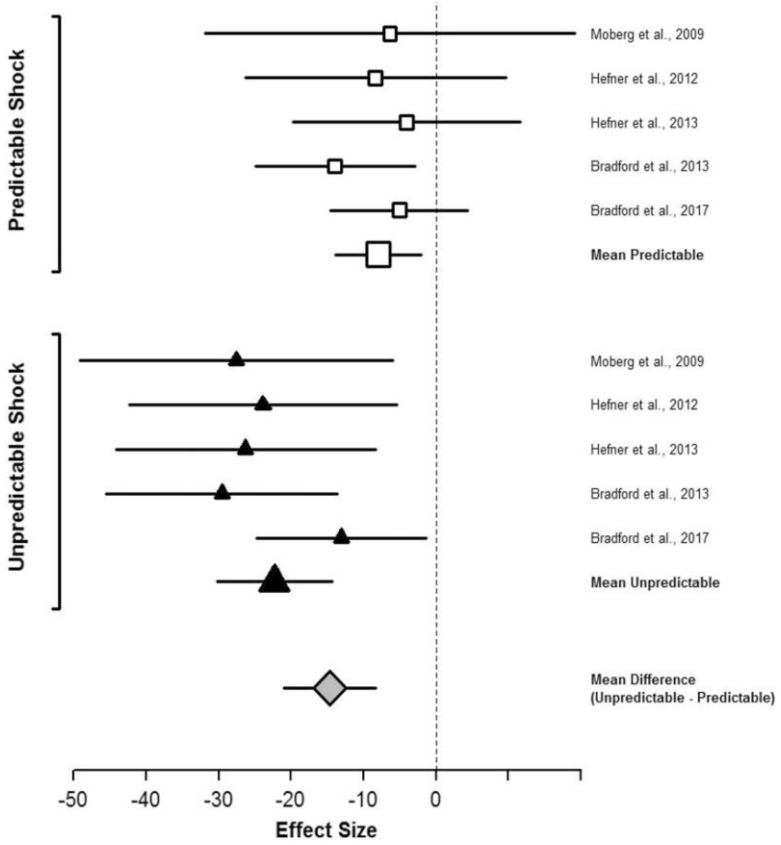

Figure 1. Acute alcohol intoxication disproportionately reduces responses to uncertain and unpredictable threat. Forest plot depicts the consequences of acute, sub-sedative alcohol administration (BAL Range = 0.061 – 0.1455) on startle potentiation during the anticipation of uncertain and certain shock delivery. On average, the anxiolytic effects of alcohol were three-fold greater for uncertain compared to certain threat. Uncertainty was manipulated using a combination of timing and probability (Moberg & Curtin, 2009; *n*=64), timing (Hefner et al., 2013; *n*=68), probability (Hefner & Curtin, 2012; *n*=120), intensity (Bradford et al., 2013; *n*=89), or somatic location of shock delivery (Bradford et al., 2017; *n*=94). Effect sizes indicate the mean difference in startle potentiation (Δ μV) across intoxicated and sober (i.e., placebo and/or no-alcohol control) groups. Error bars indicate 95% confidence intervals. Figure reproduced from Kaye et al. (2017).

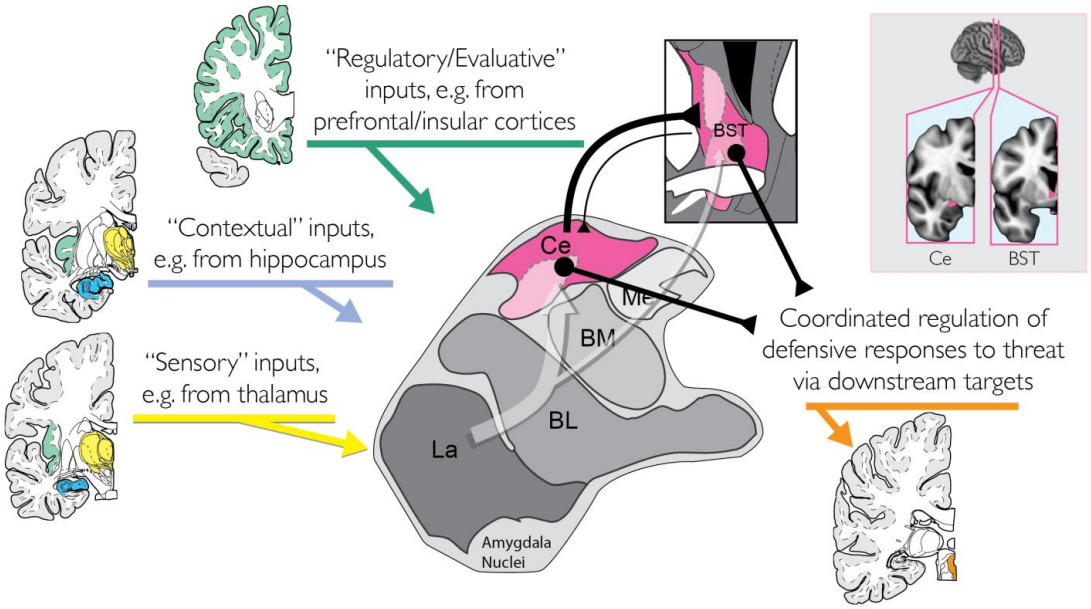

Figure 2. The central extended amygdala helps organize defensive responses to threat. Simplified schematic of key inputs and outputs to the central extended amygdala (*magenta*) in humans and other primates. The central extended amygdala encompasses the central nucleus of the amygdala (Ce), which lies in the dorsal amygdala, and the bed nucleus of the stria terminalis (BST), which wraps around the anterior commissure. As shown by the translucent white arrow at the center of the figure, much of the sensory (*yellow*), contextual (*blue*), and regulatory (*green*) inputs to the central extended amygdala are indirect (i.e., poly-synaptic), and often first pass through adjacent amygdala nuclei before arriving at the Ce or BST. In primates, projections linking the Ce with the BST are predominantly from the Ce to the BST. The Ce and BST are both poised to orchestrate or trigger momentary negative affect via projections to downstream target regions (*orange*), such as the periaqueductal grey (PAG). *Inset:* Coronal slices depicting the relative locations of the Ce and the BST (*magenta*) in the human brain. Portions of this figure were adapted with permission from (Mai et al., 2007). The BST region depicted in the inset is described in (Theiss, Ridgewell, McHugo, Heckers, & Blackford, 2017).

Abbreviations: Basolateral (BL), Basomedial (BM), Central (Ce), Lateral (La), and Medial (Me) nuclei of the amygdala; Bed nucleus of the stria terminalis (BST).

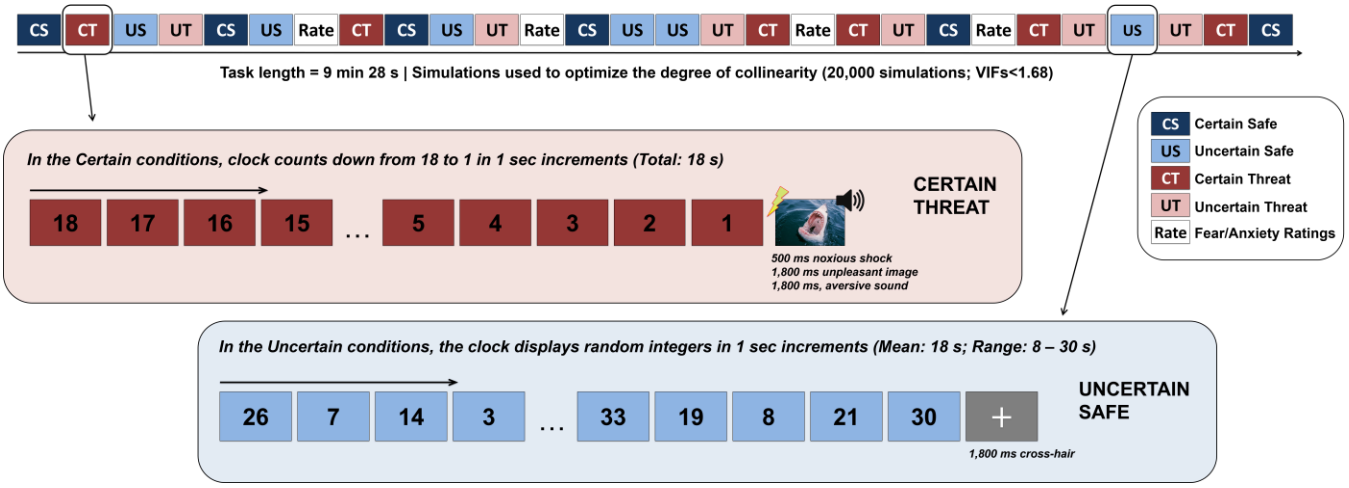

Figure 3. MultiThreat Countdown Task. Effects of temporal certainty (Certain/Uncertain) and stimulus type (Threat/Safe) were examined in a 2 × 2 factorial design. During Certain trials, integers were consistently presented in consecutive order from 18 to 0, reliably counting down the seconds until stimulus delivery. During Uncertain trials, a series of different random integers were displayed every second for a random duration (Range = 8 – 30 s, *M* = 18 s). Each trial ended with a stimulus which was either aversive (concurrent 500ms electric shock; aversive image; and frightening sound) or neutral (grey screen with white fixation). Background color during the countdown period indicated the valence condition for stimulus type (red = adverse, blue = neutral; colors matched for intensity). Each trial type occurred 6 times per run and the length of task was approximately 10 minutes. Trial order was set using modified m-sequences. Four times per run (once per condition), participants were asked to rate their anxiety during the previous trial on a scale from 1(“least”) to 4(“most”).

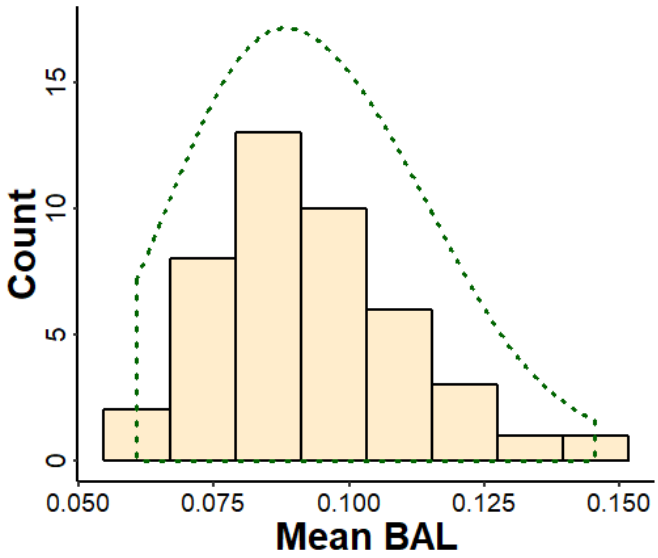

Figure 4. BAL for participants randomly assigned to the alcohol group (*n=49).* BAL was estimated using breath assays conducted immediately before and immediately after the imaging component of the session. Histogram depicts the mean of the two assessments.

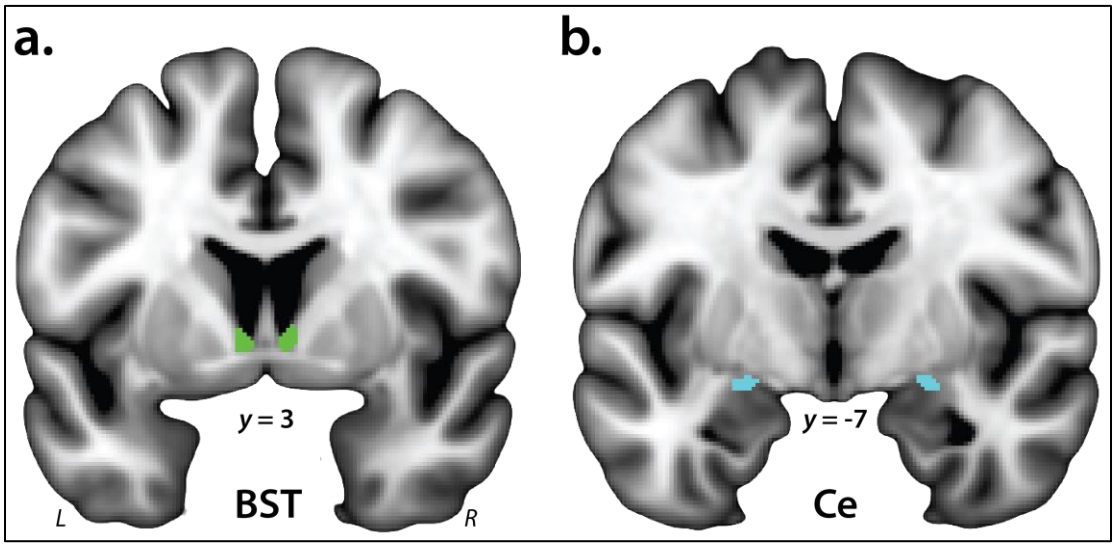

Figure 5. Bed Nucleus of the Stria Terminalis (BST) and Central Nucleus of the Amygdala (Ce) ROIs. The derivation of the probabilistic BST mask (green) is described in more detail in Theiss et al. (2016) and was thresholded at 25%. The ROI mostly encompasses the supra-commissural BST, given the difficulty of reliably discriminating the borders of regions below the anterior commissure on the basis of T1-weighted MRI (Kruger, Shiozawa, Kreifelts, Scheffler, & Ethofer, 2015). Building on prior work by our group (Birn et al., 2014; Oler et al., 2012; 2016), the Ce mask (cyan) was manually prescribed by a trained anatomist (B.M. Nacewicz) based on the atlas of Mai and colleagues (Mai et al., 2007) and using a high-resolution (0.7-mm), multi-modal (T1w/T2w) probabilistic MRI template (Tyszka & Pauli, 2016). For illustrative purposes, 1-mm masks are shown. Analyses employed ROIs decimated to the 2-mm resolution of the EPI data. Abbreviations—L, left hemisphere; R, right hemisphere.

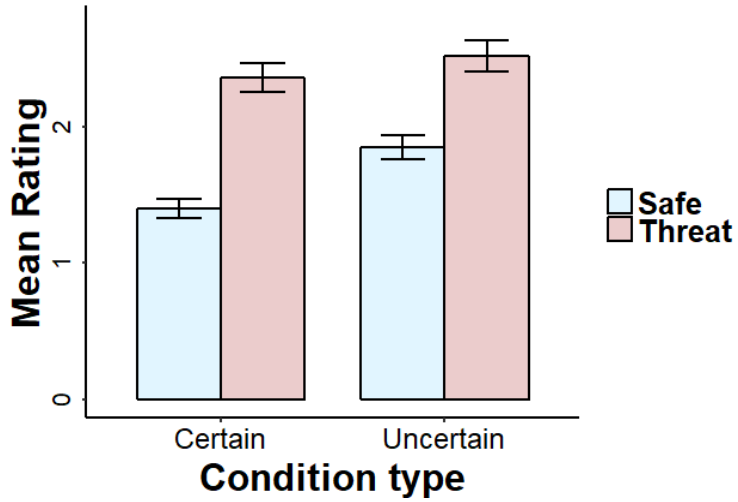

Figure 6. Subjective fear/anxiety ratings by condition. Error bars depict the standard error of the mean.

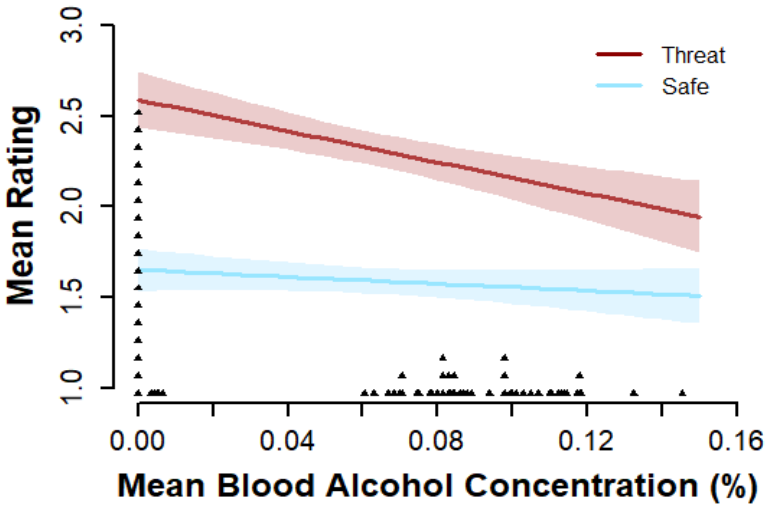

Figure 7. Subjective fear/anxiety ratings as a function of mean BAL and threat type. The dark lines represent point estimates of mean ratings from a GLM, with confidence envelopes of ±1 SE (translucent bands). The strip plot shows the mean BAL for all participants The line coefficients for Threat and Safe are -0.19 (p=.009) and -0.026 (p=0.7), respectively.

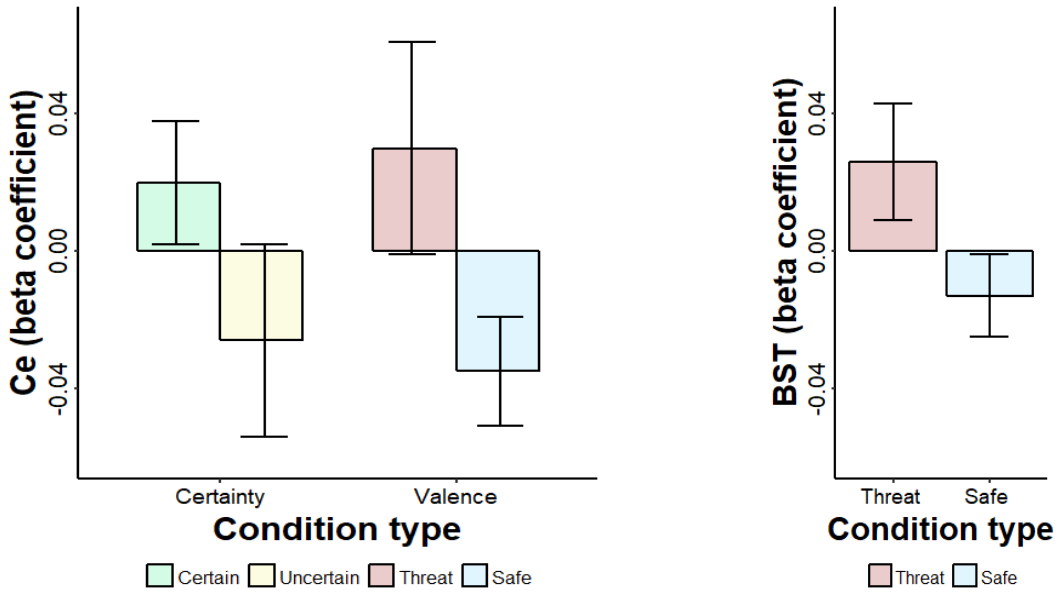

Figure 8. BOLD response beta coefficients for Ce and BST by condition. Error bars depict the standard error of the mean.

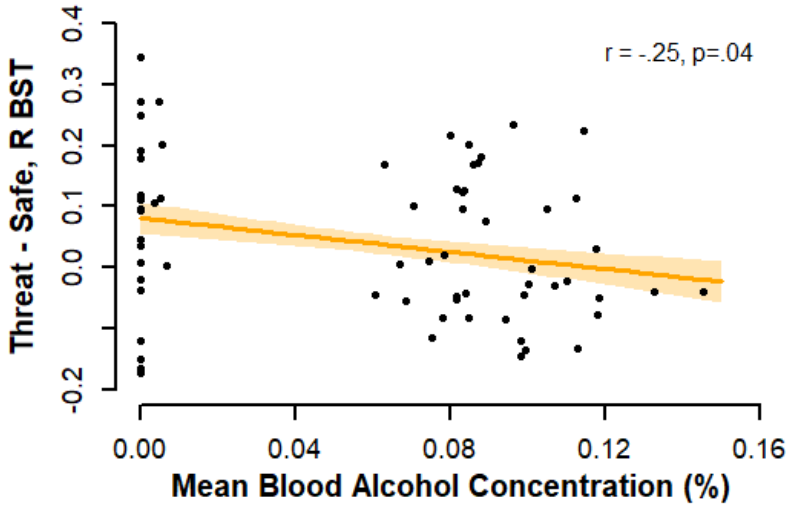

Figure 9. Valence effect (Threat > Safe) within Right BST as a function of mean BAL. The dark line represents point estimates from a GLM of the difference of beta values between Threat and Safe conditions, with confidence envelopes of ±1 SE (translucent band). The scatterplot shows observed values for all participants. The Pearson's correlation values are shown in the top right (r = -0.25, *p*=.04).

Appendix

Imaging and Ratings Sample Characteristics

Table 1b

Imaging sample characteristics (N=67)

Variable	Total	Placebo	Alcohol	*P*-value
Sample size (*N*)	67	23	44	
Age (years)	22.3 (2.19)	(22.2) 1.34	(22.3) 2.54	t(65) = 0.3, *p* = 0.8
Gender				
Female	49% (*n*=33)	48% (*n*=11)	50% (*n*=22)	z = 0.17, *p* = 0.9
Male	51% (*n*=34)	52% (*n*=12)	50% (*n*=22)	
Current Alcohol Use				
Mean drinks/week	7.12 (6.33)	(6.90) 6.00	7.23 (6.57)	t(45) = 0.2, *p* = 0.8
BAL (%)				
Prior MRI session	0.071 (0.09)	0.002 (0.00)	0.107 (0.09)	t(44) = 7.8, *p*<.001*
After MRI session	0.061 (0.05)	0.000 (0.00)	0.092 (0.02)	t(43) = 30.3, *p*<.001*

Note: Group characteristics were tested for differences using Welch's unpaired t-test to account for unequal variances between groups. Equality of gender proportions were testing using a binomial GLM.

Table 1c

Ratings sample characteristics (N=61)

Variable	Total	Placebo	Alcohol	*P*-value
Sample size (*N*)	61	19	42	
Age (years)	22.2 (2.1)	22.4 (1.38)	22.1 (2.3)	t(54) = -.6, *p* = .5
Gender				
Female	56% (*n*=34)	53% (*n*=10)	57% (*n*=24)	z = -.33, *p* = 0.7
Male	44% (*n*=27)	47% (*n*=9)	43% (*n*=18)	
Current Alcohol Use				
Mean drinks/week	7.13 (6.05)	5.50 (2.92)	7.86 (6.93)	t(59) = 1.9, *p* = 0.07
BAL (%)				
Prior MRI session	0.075 (0.09)	0.002 (0.00)	0.107 (.09)	t(41) = 7.5, *p*<.001*
After MRI session	0.063 (0.05)	0.00 (0.00)	0.091 (.02)	t(41) = 28.1, *p*<.001*

Note: Group characteristics were tested for differences using Welch's unpaired t-test to account for unequal variances between groups. Equality of gender proportions were testing using a binomial GLM.

References

Alvarez, R. P., Chen, G., Bodurka, J., Kaplan, R., & Grillon, C. (2011). Phasic and sustained fear in humans elicits distinct patterns of brain activity. *Neuroimage, 55*, 389-400. doi:10.1016/j.neuroimage.2010.11.057

Andreatta, M., Glotzbach-Schoon, E., Muhlberger, A., Schulz, S. M., Wiemer, J., & Pauli, P. (2015). Initial and sustained brain responses to contextual conditioned anxiety in humans. *Cortex, 63*, 352-363. doi:10.1016/j.cortex.2014.09.014

Asok, A., Schulkin, J., & Rosen, J. B. (2017). Corticotropin releasing factor type-1 receptor antagonism in the dorsolateral bed nucleus of the stria terminalis disrupts contextually conditioned fear, but not unconditioned fear to a predator odor. *Psychoneuroendocrinology, 70*, 17-24. doi:10.1016/j.psyneuen.2016.04.021

Atlas, L. Y., Bolger, N., Lindquist, M. A., & Wager, T. D. (2010). Brain mediators of predictive cue effects on perceived pain. *Journal of Neuroscience, 30*, 12964-12977.

Avants, B. B., Tustison, N. J., Song, G., Cook, P. A., Klein, A., & Gee, J. C. (2011). A reproducible evaluation of ANTs similarity metric performance in brain image registration. *Neuroimage, 54*, 2033-2044. doi:10.1016/j.neuroimage.2010.09.025

Avery, S. N., Clauss, J. A., & Blackford, J. U. (2016). The human BNST: Functional role in anxiety and addiction. *Neuropsychopharmacology, 41*, 126-141. doi:10.1038/npp.2015.185

Baas, J. M., Grillon, C., Bocker, K. B., Brack, A. A., Morgan, C. A., 3rd, Kenemans, J. L., & Verbaten, M. N. (2002). Benzodiazepines have no effect on fear-potentiated startle in humans. *Psychopharmacology, 161*, 233-247. doi:10.1007/s00213-002-1011-8

Birn, R. M., Shackman, A. J., Oler, J. A., Williams, L. E., McFarlin, D. R., Rogers, G. M., . . . Kalin, N. H. (2014). Extreme early-life anxiety is associated with an evolutionarily conserved reduction in the strength of intrinsic functional connectivity between the dorsolateral prefrontal cortex and the central nucleus of the amygdala. *Molecular Psychiatry, 19*, 853. doi:10.1038/mp.2014.85

Bjork, J. M., & Gilman, J. M. (2014). The effects of acute alcohol administration on the human brain: Insights from neuroimaging. *Neuropharmacology, 0*, 101-110. doi:10.1016/j.neuropharm.2013.07.039

Botta, P., Demmou, L., Kasugai, Y., Markovic, M., Xu, C., Fadok, J. P., . . . Luthi, A. (2015). Regulating anxiety with extrasynaptic inhibition. *Nature Neuroscience, 18*, 1493-1500. doi:10.1038/nn.4102

Bradford, D. E., Shapiro, B. L., & Curtin, J. J. (2013). How bad could it be? Alcohol dampens stress responses to threat of uncertain intensity. *Psychol Sci, 24*, 2541-2549. doi:10.1177/0956797613499923

Breese, G. R., Criswell, H. E., Carta, M., Dodson, P. D., Hanchar, H. J., Khisti, R. T., . . . Wallner, M. (2006). Basis of the Gabamimetic Profile of Ethanol. *Alcoholism: Clinical and Experimental Research, 30*(4), 731-744. doi:10.1111/j.0145-6008.2006.00086.x

Brinkmann, L., Buff, C., Neumeister, P., Tupak, S. V., Becker, M. P., Herrmann, M. J., & Straube, T. (2017). Dissociation between amygdala and bed nucleus of the stria terminalis during threat anticipation in female post-traumatic stress disorder patients. *Human Brain Mapping, 38*, 2190-2205. doi:10.1002/hbm.23513

Buchanan, T. W., Tranel, D., & Adolphs, R. (2004). Anteromedial temporal lobe damage blocks startle modulation by fear and disgust. *Behavioral Neuroscience, 118*(2), 429-437. doi:10.1037/0735-7044.118.2.429 [doi]
2004-12681-020 [pii]

Chung, M. K., Worsley, K. J., Nacewicz, B. M., Dalton, K. D., & Davidson, R. J. (2010). General multivariate linear modeling of surface shapes using SurfStat. *Neuroimage, 53*, 491-505.

Cooper, M. L. (1994). Motivations for alcohol use among adolescents: Development and validation of a four-factor model. *Psychological Assessment, 6*(2), 117-128. doi:10.1037/1040-3590.6.2.117

Cox, R. W. (1996). AFNI: Software for analysis and visualization of functional magnetic resonance neuroimages. *Computers and Biomedical Research, 29*, 162-173. doi:10.1006/cbmr.1996.0014

Curtin, J. J., & Fairchild, B. A. (2003). Alcohol and cognitive control: Implications for regulation of behavior during response conflict. *Journal of Abnormal Psychology, 112*(3), 424-436.

Davis, M. (1998). Are different parts of the extended amygdala involved in fear versus anxiety? *Biological Psychiatry, 44*, 1239-1247.

Davis, M. (2000). The role of the amygdala in conditioned and unconditioned fear and anxiety. In J. P. Aggleton (Ed.), *The amygdala: A functional analysis (2nd ed)* (pp. 213–287). Oxford: Oxford University Press.

Davis, M. (2006). Neural systems involved in fear and anxiety measured with fear-potentiated startle. *American Psychologist, 61*, 741-756. doi:10.1037/0003-066X.61.8.741

Davis, M., Walker, D. L., Miles, L., & Grillon, C. (2010). Phasic vs sustained fear in rats and humans: Role of the extended amygdala in fear vs anxiety. *Neuropsychopharmacology, 35*, 105-135. doi:10.1038/npp.2009.109

Duvarci, S., Bauer, E. P., & Paré, D. (2009). The bed nucleus of the stria terminalis mediates inter-individual variations in anxiety and fear. *Journal of Neuroscience, 29*, 10357-10361. doi:10.1523/jneurosci.2119-09.2009

Excessive Drinking is Draining the U.S. Economy. (2016, January 12, 2016). Retrieved from https://www.cdc.gov/features/costsofdrinking/index.html

Fadda, F., & Rossetti, Z. L. (1998). Chronic ethanol consumption: from neuroadaptation to neurodegeneration. *Progress in Neurobiology, 54*(4), 385-431.

Fox, A. S., Lapate, R. C., Shackman, A. J., & Davidson, R. J. (*in press*). The psychological and neurobiological bases of dispositional negativity. In A. S. Fox, R. C. Lapate, A. J. Shackman, & R. J. Davidson (Eds.), *The nature of emotion. Fundamental questions* (2nd ed.). New York: Oxford University Press.

Funayama, E. S., Grillon, C., Davis, M., & Phelps, E. A. (2001). A double dissociation in the affective modulation of startle in humans: effects of unilateral temporal lobectomy. *Journal of Cognitive Neuroscience, 13*(6), 721-729. doi:10.1162/08989290152541395 [doi]

Gilpin, N. W., & Koob, G. F. (2008). Neurobiology of alcohol dependence: focus on motivational mechanisms. *Alcohol Research and Health, 31*(3), 185-195.

Gorka, S. M., Lieberman, L., Shankman, S. A., & Phan, K. L. (2017). Association between neural reactivity and startle reactivity to uncertain threat in two independent samples. *Psychophysiology*. doi:10.1111/psyp.12829

Greve, D. N., & Fischl, B. (2009). Accurate and robust brain image alignment using boundary-based registration. *Neuroimage, 48*, 63-72.

Grillon, C., Baas, J. M., Cornwell, B., & Johnson, L. (2006). Context conditioning and behavioral avoidance in a virtual reality environment: effect of predictability. *Biological Psychiatry, 60*(7), 752-759. doi:10.1016/j.biopsych.2006.03.072 [doi]

Grillon, C., Baas, J. M., Pine, D. S., Lissek, S., Lawley, M., Ellis, V., & Levine, J. (2006). The benzodiazepine alprazolam dissociates contextual fear from cued fear in humans as assessed by fear-potentiated startle. *Biological Psychiatry, 60*(7), 760-766. doi:10.1016/j.biopsych.2005.11.027

Grupe, D. W., & Nitschke, J. B. (2013). Uncertainty and anticipation in anxiety: an integrated neurobiological and psychological perspective. *Nature Reviews. Neuroscience, 14*, 488-501. doi:10.1038/nrn3524

Grupe, D. W., Oathes, D. J., & Nitschke, J. B. (2013). Dissecting the anticipation of aversion reveals dissociable neural networks. *Cerebral Cortex, 23*, 1874-1883. doi:10.1093/cercor/bhs175

Gungor, N. Z., & Paré, D. (2016). Functional heterogeneity in the bed nucleus of the stria terminalis. *Journal of Neuroscience, 36*, 8038-8049.

Hefner, K. R., & Curtin, J. J. (2012). Alcohol stress response dampening: selective reduction of anxiety in the face of uncertain threat. *J Psychopharmacol, 26*(2), 232-244. doi:10.1177/0269881111416691

Hefner, K. R., Moberg, C. A., Hachiya, L. Y., & Curtin, J. J. (2013). Alcohol stress response dampening during imminent versus distal, uncertain threat. *Journal of Abnormal Psychology, 122*(3), 756-769. doi:10.1037/a0033407

Herman, M. A., Kallupi, M., Luu, G., Oleata, C. S., Heilig, M., Koob, G. F., . . . Roberto, M. (2013). Enhanced GABAergic transmission in the central nucleus of the amygdala of genetically selected Marchigian Sardinian rats: alcohol and CRF effects. *Neuropharmacology, 67*, 337-348. doi:10.1016/j.neuropharm.2012.11.026

Herrmann, M. J., Boehme, S., Becker, M. P., Tupak, S. V., Guhn, A., Schmidt, B., . . . Straube, T. (2016). Phasic and sustained brain responses in the amygdala and the bed nucleus of the stria terminalis during threat anticipation. *Human Brain Mapping, 37*, 1091-1102. doi:10.1002/hbm.23088

Jennings, J. H., Sparta, D. R., Stamatakis, A. M., Ung, R. L., Pleil, K. E., Kash, T. L., & Stuber, G. D. (2013). Distinct extended amygdala circuits for divergent motivational states. *Nature, 496*, 224-228. doi:nature12041 [pii]
10.1038/nature12041

Kaye, J. T., Bradford, D. E., Magruder, K. P., & Curtin, J. J. (2017). Probing for Neuroadaptations to Unpredictable Stressors in Addiction: Translational Methods and Emerging Evidence. *Journal of Studies on Alcohol and Drugs, 78*(3), 353-371.

Kim, S. Y., Adhikari, A., Lee, S. Y., Marshel, J. H., Kim, C. K., Mallory, C. S., . . . Deisseroth, K. (2013). Diverging neural pathways assemble a behavioural state from separable features in anxiety. *Nature, 496*, 219-223. doi: 10.1038/nature12018

Klumpers, F., Kroes, M. C., Heitland, I., Everaerd, D., Akkermans, S. E., Oosting, R. S., . . . Baas, J. M. (2015). Dorsomedial prefrontal cortex mediates the impact of serotonin transporter linked polymorphic region genotype on anticipatory threat reactions. *Biological Psychiatry, 78*, 582-589. doi:10.1016/j.biopsych.2014.07.034

Koob, G. F. (2004). A role for GABA mechanisms in the motivational effects of alcohol. *Biochemical Pharmacology, 68*(8), 1515-1525. doi:10.1016/j.bcp.2004.07.031

Koob, G. F. (2008). A role for brain stress systems in addiction. *Neuron, 59*(1), 11-34. doi:10.1016/j.neuron.2008.06.012

Koob, G. F. (2010). Focus on: Neuroscience and treatment: the potential of neuroscience to inform treatment. *Alcohol Research and Health, 33*(1-2), 144-151.

Kruger, O., Shiozawa, T., Kreifelts, B., Scheffler, K., & Ethofer, T. (2015). Three distinct fiber pathways of the bed nucleus of the stria terminalis to the amygdala and prefrontal cortex. *Cortex, 66*, 60-68. doi:10.1016/j.cortex.2015.02.007

Kumar, S., Porcu, P., Werner, D. F., Matthews, D. B., Diaz-Granados, J. L., Helfand, R. S., & Morrow, A. L. (2009). The role of GABA(A) receptors in the acute and chronic effects of ethanol: a decade of progress. *Psychopharmacology, 205*(4), 529-564. doi:10.1007/s00213-009-1562-

Lang, P. J., Bradley, M. M., & Cuthbert, B. N. (2008). *International affective picture system (IAPS): Affective ratings of pictures and instruction manual. Technical Report A-8*. Retrieved from Gainesville, FL:

Lebow, M. A., & Chen, A. (*in press*). Overshadowed by the amygdala: the bed nucleus of the stria terminalis emerges as key to psychiatric disorders. *Molecular Psychiatry*. doi:10.1038/mp.2016.1

LeDoux, J. E. (2015). *Anxious. Using the brain to understand and treat fear and anxiety*. NY: Viking.

Leriche, M., Méndez, M., Zimmer, L., & Bérod, A. (2008). Acute ethanol induces Fos in GABAergic and non-GABAergic forebrain neurons: A double-labeling study in the medial prefrontal cortex and extended amygdala. *Journal of Neuroscience, 153*(1), 259-267. doi:10.1016/j.neuroscience.2008.01.069

Lieberman, L., Gorka, S. M., Shankman, S. A., & Phan, K. L. (2017). Impact of panic on psychophysiological and neural reactivity to unpredictable threat in depression and anxiety. *Clin Psychol Sci, 5*(1), 52-63. doi:10.1177/2167702616666507

Lim, S. L., Padmala, S., & Pessoa, L. (2009). Segregating the significant from the mundane on a moment-to-moment basis via direct and indirect amygdala contributions. *Proceedings of the National Academy of Sciences of the United States of America, 106*, 16841-16846. doi:10.1073/pnas.0904551106

Lindquist, M. A., Loh, J. M., Atlas, L. Y., & Wager, T. D. (2009). Modeling the Hemodynamic Response Function in fMRI: Efficiency, Bias and Mis-modeling. *Neuroimage, 45*(1 Suppl), S187-S198. doi:10.1016/j.neuroimage.2008.10.065

Mai, J. K., Majtanik, M., & Paxinos, G. (2015). *Atlas of the human brain* (4th ed.). San Diego, CA: Academic Press.

Mai, J. K., Paxinos, G., & Voss, T. (2007). *Atlas of the human brain* (3rd ed.). San Diego, CA: Academic Press.

Mann, L. M., Chassin, L., & Sher, K. J. (1987). Alcohol expectancies and the risk for alcoholism. *Journal of Consulting and Clinical Psychology, 55*(3), 411-417.

McMenamin, B. W., Langeslag, S. J., Sirbu, M., Padmala, S., & Pessoa, L. (2014). Network organization unfolds over time during periods of anxious anticipation. *Journal of Neuroscience, 34*, 11261-11273. doi:10.1523/jneurosci.1579-14.2014

Moberg, C. A., & Curtin, J. J. (2009). Alcohol selectively reduces anxiety but not fear: Startle response during unpredictable vs. predictable threat. *J Abnormal Psychol, 118*, 335-347.

Moberg, C. A., & Curtin, J. J. (2012). Stressing the importance of anxiety in alcoholism. *Alcoholism: Clinical and Experimental Research, 36*, 60A.

Moreira, C. M., Masson, S., Carvalho, M. C., & Brandao, M. L. (2007). Exploratory behavior of rats in the elevated plus maze is differentially sensitive to inactivation of the basolateral and central amygdaloid nuclei. *Brain Research Bulletin, 71*, 466-474.

Nacewicz, B. M., Alexander, A. L., Kalin, N. H., & Davidson, R. J. (2014). The neurochemical underpinnings of human amygdala volume including subregional contributions. *Biological Psychiatry, 75*, S222.

Nacewicz, B. M., Dalton, K. M., Johnstone, T., Long, M. T., McAuliff, E. M., Oakes, T. R., . . . Davidson, R. J. (2006). Amygdala Volume and Nonverbal Social Impairment in Adolescent and Adult Males With Autism. *Archives of General Psychiatry, 63*, 1417-1428.

Oler, J. A., Birn, R. M., Patriat, R., Fox, A. S., Shelton, S. E., Burghy, C. A., . . . Kalin, N. H. (2012). Evidence for coordinated functional activity within the extended amygdala of non-human and human primates. *Neuroimage, 61*, 1059-1066.

Oler, J. A., Tromp, D. P., Fox, A. S., Kovner, R., Davidson, R. J., Alexander, A. L., . . . Fudge, J. L. (2017). Connectivity between the central nucleus of the amygdala and the bed nucleus of the stria terminalis in the non-human primate: neuronal tract tracing and developmental neuroimaging studies. *Brain Struct Funct, 222*, 21-39. doi:10.1007/s00429-016-1198-9

Page, M. C., Braver, S. L., & MacKinnon, D. P. (2003). *Levine's guide to SPSS for analysis of variance (2nd ed.)*. Mahwah, NJ, US: Lawrence Erlbaum Associates Publishers.

Paul, S. M. (2006). Alcohol-sensitive GABA receptors and alcohol antagonists. *Proceedings of the National Academy of Sciences, 103*(22), 8307-8308. doi:10.1073/pnas.0602862103

Paulus, M. P., Feinstein, J. S., Castillo, G., Simmons, A. N., & Stein, M. B. (2005). Dose-dependent decrease of activation in bilateral amygdala and insula by lorazepam during emotion processing. *Archives of General Psychiatry, 62*, 282-288. doi:10.1001/archpsyc.62.3.282

Paxinos, G., Huang, X., Petrides, M., & Toga, A. (2009). *The rhesus monkey brain in stereotaxic coordinates* (2nd ed.). San Diego: Academic Press.

Paxinos, G., & Watson, C. (2014). *The rat brain in stereotaxic coordinates* (7th ed.). Sand Diego, CA: Academic Press.

Petrakis, I. L., Gonzalez, G., Rosenheck, R., & Krystal, J. H. (2002). Comorbidity of Alcholism and Psychiatric Disorders: An Overview. *Alcohol Research, 26*(2), 81.

Prevost, C., McCabe, J. A., Jessup, R. K., Bossaerts, P., & O'Doherty, J. P. (2011). Differentiable contributions of human amygdalar subregions in the computations underlying reward and avoidance learning. *European Journal of Neuroscience, 34*, 134-145. doi:10.1111/j.1460-9568.2011.07686.x

Roberto, M., Madamba, S. G., Moore, S. D., Tallent, K. A., & Siggins, G. R. (2003). Ethanol increases GABAergic transmission at both pre- and postsynaptic sites in rat central amygdala neurons. *PNAS, 100*(4), 2053-2058. doi:10.1073/pnas.0437926100

RStudioTeam. RStudio: Integrated Development for R (Version 1.0.143). Boston, MA: RStudio, Inc. at <http://www.rstudio.com/>.

Schmidt, N. B., Buckner, J. D., & Keough, M. E. (2007). Anxiety sensitivity as a prospective predictor of alcohol use disorders. *Behav Modif., 31*(2), 202-219.

Schroder, K. E., & Perrine, M. W. (2007). Covariations of emotional states and alcohol consumption: evidence from 2 years of daily data collection. *Social Science & Medicine, 65*(12), 2588-2602.

Shackman, A. J., & Fox, A. S. (2016). Contributions of the central extended amygdala to fear and anxiety. *Journal of Neuroscience, 36*, 8050-8063. doi:10.1523/jneurosci.0982-16.2016

Shackman, A. J., Kaplan, C. M., Stockbridge, M. D., Tillman, R. M., Tromp, D. P. M., Fox, A. S., & Gamer, M. (2016). The neurobiology of anxiety and attentional biases to threat: Implications for understanding anxiety disorders in adults and youth. *Journal of Experimental Psychopathology, 7*, 311-342.

Shackman, A. J., Sarinopoulos, I., Maxwell, J. S., Pizzagalli, D. A., Lavric, A., & Davidson, R. J. (2006). Anxiety selectively disrupts visuospatial working memory. *Emotion, 6*, 40-61.

Silberman, Y., & Winder, D. G. (2015). Ethanol and Corticotropin Releasing Factor Receptor Modulation of Central Amygdala Neurocircuitry: an Update and Future Directions. *Alcohol (Fayetteville, N.Y.), 49*(3), 179-184. doi:10.1016/j.alcohol.2015.01.006

Smith, J. P., & Randall, C. L. (2012). Anxiety and Alcohol Use Disorders: Comorbidity and Treatment Considerations. *Alcohol Res, 34*(4), 414-431.

Smith, K. (2014). Mental health: a world of depression. *Nature, 515*, 181. doi:10.1038/515180a

Smith, S. M., Jenkinson, M., Woolrich, M. W., Beckmann, C. F., Behrens, T. E. J., Johansen-Berg, H., . . . Matthews, P. M. (2004). Advances in functional and structural MR image analysis and implementation as FSL. *Neuroimage, 23*, S208-S219. doi:10.1016/j.neuroimage.2004.07.051

Sobell, L. C., Agrawal S Fau - Sobell, M. B., Sobell Mb Fau - Leo, G. I., Leo Gi Fau - Young, L. J., Young Lj Fau - Cunningham, J. A., Cunningham Ja Fau - Simco, E. R., & Simco, E. R. (2003). Comparison of a quick drinking screen with the timeline followback for individuals with alcohol problems. *Journal of Studies on Alcohol, 64*(6), 858-861.

Somerville, L. H., Wagner, D. D., Wig, G. S., Moran, J. M., Whalen, P. J., & Kelley, W. M. (2013). Interactions between transient and sustained neural signals support the generation and regulation of anxious emotion. *Cerebral Cortex, 23*, 49-60. doi:10.1093/cercor/bhr373

Sripada, C. S., Angstadt, M., McNamara, P., King, A. C., & Phan, K. L. (2011). Effects of alcohol on brain responses to social signals of threat in humans. *Neuroimage, 55*(1), 371-380. doi:10.1016/j.neuroimage.2010.11.062

Sun, N., & Cassell, M. D. (1993). Intrinsic GABAergic neurons in the rat central extended amygdala. *The Journal of Comparative Neurology, 330*(3), 381-404. doi:10.1002/cne.903300308

Theiss, J. D., Ridgewell, C., McHugo, M., Heckers, S., & Blackford, J. U. (2016). Manual segmentation of the human bed nucleus of the stria terminalis using 3T MRI. *Neuroimage, 146*, 288-292. doi:10.1016/j.neuroimage.2016.11.047

Theiss, J. D., Ridgewell, C., McHugo, M., Heckers, S., & Blackford, J. U. (2017). Manual segmentation of the human bed nucleus of the stria terminalis using 3T MRI. *Neuroimage, 146*, 288-292. doi:10.1016/j.neuroimage.2016.11.047

Tovote, P., Fadok, J. P., & Luthi, A. (2015). Neuronal circuits for fear and anxiety. *Nature Reviews. Neuroscience, 16*, 317-331. doi:10.1038/nrn3945

Tustison, N. J., Avants, B. B., Cook, P. A., Zheng, Y. J., Egan, A., Yushkevich, P. A., & Gee, J. C. (2010). N4ITK: Improved N3 bias correction. *IEEE Transactions on Medical Imaging, 29*, 1310-1320. doi:10.1109/tmi.2010.2046908

Tyszka, J. M., & Pauli, W. M. (2016). In vivo delineation of subdivisions of the human amygdaloid complex in a high-resolution group template. *Human Brain Mapping, 37*, 3979-3998. doi:10.1002/hbm.23289

Walker, D., Yang, Y., Ratti, E., Corsi, M., Trist, D., & Davis, M. (2009). Differential Effects of the CRF-R1 Antagonist GSK876008 on Fear-Potentiated, Light- and CRF-Enhanced Startle Suggest Preferential Involvement in Sustained versus Phasic Threat Responses. *Neuropsychopharmacology : official publication of the American College of Neuropsychopharmacology, 34*(6), 1533-1542. doi:10.1038/npp.2008.210

Wendt, J., Lotze, M., Weike, A. I., Hosten, N., & Hamm, A. O. (2008). Brain activation and defensive response mobilization during sustained exposure to phobia-related and other affective pictures in spider phobia. *Psychophysiology, 45*(2), 205-215. doi:10.1111/j.1469-8986.2007.00620.x

Williams, L. E., Oler, J. A., Fox, A. S., McFarlin, D. R., Rogers, G. M., Jesson, M. A., . . . Kalin, N. H. (2015). Fear of the unknown: Uncertain anticipation reveals amygdala alterations in childhood anxiety disorders. *Neuropsychopharmacology, 40*, 1428-1435. doi:10.1038/npp.2014.328

Yoo, T. S., Ackerman Mj Fau - Lorensen, W. E., Lorensen We Fau - Schroeder, W., Schroeder W Fau - Chalana, V., Chalana V Fau - Aylward, S., Aylward S Fau - Metaxas, D., . . . Whitaker, R. (2002). Engineering and algorithm design for an image processing Api: a technical report on ITK--the Insight Toolkit. *Studies in Health Technology and Informatics, 85*, 586-592.

Zimmerman, J. M., & Maren, S. (2011). The bed nucleus of the stria terminalis is required for the expression of contextual but not auditory freezing in rats with basolateral amygdala lesions. *Neurobiology of Learning and Memory, 95*, 199-205. doi:10.1016/j.nlm.2010.11.002

Zimmerman, J. M., Rabinak, C. A., McLachlan, I. G., & Maren, S. (2007). The central nucleus of the amygdala is essential for acquiring and expressing conditional fear after overtraining. *Learning and Memory, 14*, 634-644. doi:10.1101/lm.607207

Zimmerman, P., Wittchen, H. U., Höfler, M., Pfister, H., Kessler, R. C., & Lieb, R. (2003). Primary anxiety disorders and the development of subsequent alcohol use disorders: a 4-year community study of adolescents and young adults. *Psychological Medicine, 33*(7), 1211-1222.